Development of true-stress creep model through analysis of constant-load creep data with application to finite element methods

Martin Connolly*, Mark Whittaker*, Steve Williams^

*Department of Engineering, Swansea University, ^Rolls-Royce Plc.

1. Abstract

The creep behaviour of the nickel-superalloy RR1000 is studied through a number of constant-load creep tests. It is often assumed that creep data generated by constant-load testing are unsuitable for building a generalised creep model due to the non-constant stresses incurred. Analysis of existing models shows that significant errors may occur in many approaches, which attempt to recreate the strain evolution with time. A model is presented which is not reliant on time as a parameter and is therefore able to utilise constant-load creep data without enforcing the assumption of a constant stress. This model is demonstrated through numerical analyses to replicate the creep behaviour across a large range of stresses accurately. The proposed model is then adapted as an Abaqus™ user-subroutine to demonstrate capability within finite element analysis.

2. Introduction

Nickel superalloys are often chosen for applications where a combination of high temperature and high stress is anticipated. In order to achieve efficient component design, it is necessary to accurately model the behaviour of components in this extreme environment. Under such conditions, components can be expected to undergo creep deformation, which can result in a changing geometry during the life of the component. These changes can be modelled using finite element analyses provided an appropriate creep model can be applied to describe the evolution of material strain as a function of time.

Creep testing is often performed with a constant applied load. The effect of maintaining a constant load throughout the duration of a test is that the applied stress increases monotonically with accumulated strain. This is regularly considered negligible when producing a creep model for typical applications where creep strain is limited by design. However, by neglecting this effect, any model based on constant-load creep data is tied to the bulk behaviour of the test specimen, rather than providing a geometrically independent representation of the material behaviour.

Generating creep data under constant stress conditions allows for the removal of this problem. However, materials currently in service may have been described by models based on data generated under constant load conditions. It is not economical to repeat a set of existing tests in order to improve accuracy for high strain events when limited benefit would be provided for the majority of engineering cases.

There are a number of creep models available in the literature which describe the creep behaviour of nickel alloys, which are both mechanistic and empirical in derivation. A number of these models use time as a parameter[1-4], and as a result require constant stress creep data to provide a consistent

representation of the creep behaviour. The requirement for constant stress data is derived from the fact that the models described require a constant stress as an input. Constant-load tests, which produce a non-constant stress are therefore unsuitable and should not be used for such analyses.

A commonly used power-law based representation[5] provides a means to determine the change of steady-state creep rate with stress, independent of the time at condition. However, some materials, including nickel superalloys, only demonstrate a transition from primary to tertiary, with only a momentary minimum creep rate [6-8].

More recently, work has been undertaken to describe the creep behaviour under the assumption of a varying stress during a constant load creep test. A time independent creep formulation was produced[9] by combining a continuum damage mechanics (CDM) based damage parameter with the Norton power law. A CDM based model, designed to replicate different types of damage and therefore the evolution of the microstructure during creep is proposed[10]. This approach is shown to allow the production of accurate creep behaviour under both constant stress/load, without requiring assumptions to be made, such as whether to use strain or time hardening. Another approach[11] demonstrated a formulation capable of replicating the change in microstructure due to heat treatments, and the resulting creep properties of a nickel alloy (C263).

The method of power law creep typically uses a reference creep strain at which the creep rate is defined, for example the minimum rate. This means that the strain rate is defined as a function of stress alone. In order for a full creep curve to be generated from this type of model, additional terms must be applied to introduce primary and tertiary behaviours. As the alloy RR1000 does not demonstrate a significant secondary creep behaviour, the proposed model attempts to model the creep rate evolution directly as a function of both stress and strain.

This paper presents a method for generating a true-stress creep model from a set of constant-load creep data, which will allow consistent large strain creep behaviour to be recreated without requiring detailed knowledge of the material microstructure. This model is then adapted for use with the finite element package Abaqus™ for more general application.

3. Experimental Method

A number of creep tests were performed on the nickel-base superalloy RR1000 using material provided by Rolls-Royce plc. The data used for this study was produced in creep tests performed at a temperature of 700°C, as the focus was on interpreting engineering stress results to produce a true stress model. The specimens were machined to a design with a gauge length of 25.3mm and a nominal gauge section diameter of 5mm. At each end of the gauge length, a ridge was machined to allow for secure attachment of the extensometer cages, see Figure 1.

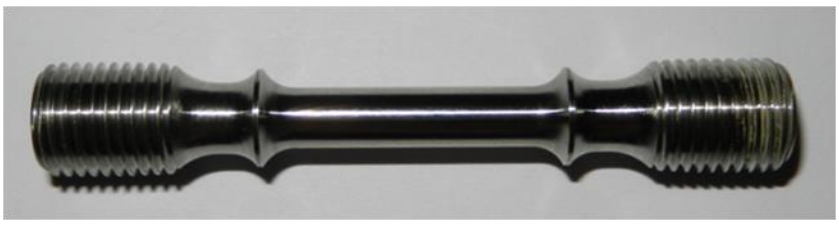

Figure 1 - Photograph of unused creep specimen

The creep tests were performed on constant-load cantilever creep rigs with a cam ratio of 10:1. The applied stress was calculated and corrected to account for the thermal expansion of the specimen during heating. This correction was applied, as it can be demonstrated that for the temperatures used in this study the change in cross-sectional area approaches 2%. Contrasting this to the requirement in the British standard for uniaxial creep testing[12], that the applied load must be known to within 1%, suggests that this is an effect that should be noted.

The creep data were analysed to calculate the evolution of the true-stress and true-strain rate with time. The true-stress was calculated based on the assumption of incompressibility during inelastic strain. This assumption leads to equation (1), where e_{EL} and e_c are the elastic and creep components of the engineering strain and S and σ are the engineering and true stresses. The Poisson's ratio of the material is represented by v. Values of 180 GPa for the elastic modulus and 0.37 for the Poisson's ratio at 700°C were taken from the Rolls-Royce materials database.

$$\sigma = \frac{S}{\left[1 - \nu e_{El} - \left(1 - \sqrt{\frac{1}{1+e_c}}\right)\right]^2} \quad (1)$$

The strain rate was calculated using the slope function in Microsoft Excel to calculate the rate at which the true strain changes with time. The true strain was calculated according to equation (2). The symbols e_t and ε_t represent the total engineering and true strain measures. Unless otherwise stated, any future reference to stress or strain within this paper should be taken to mean the true values. The true stresses and strains were calculated in this way to ensure full consistency with Abaqus™.

$$\varepsilon_t = \ln(1 + e_t) \quad (2)$$

4. Model development

4.1 Stress-Strain Rate Relationship

Figure 2 demonstrates strain rate values as a function of applied stress at two distinct values of creep strain. The values shown are measured at the points of 1% and 9.8% creep strain, from a series of constant-load creep tests at 700°C. A least squares fit for each dataset is also provided to demonstrate the linear relation between stress and the log of the strain rate. A similar relation has previously been shown[3] in the single crystal nickel-base superalloy CMSX-10.

The values in Figure 2 demonstrate how the relationship of the strain rate to applied stress varies with strain. For lower stresses, this shows the strain rate increases with strain. This is the normal behaviour for a creep test, whereby after primary creep has completed the strain rate will accelerate to failure if the stress is held constant. However, for the higher stresses, a strain hardening behaviour is presented, where for a constant stress the strain rate will decrease with accumulated strain.

For the highest stress tests shown in Figure 2, the strain hardening effect does not produce a creep curve with a decreasing rate. This is because the effect of the stress increase due to strain accumulation is greater than the strain hardening effect seen in these tests. It is likely that a constant stress test performed at these conditions would result in a creep curve with a decreasing rate.

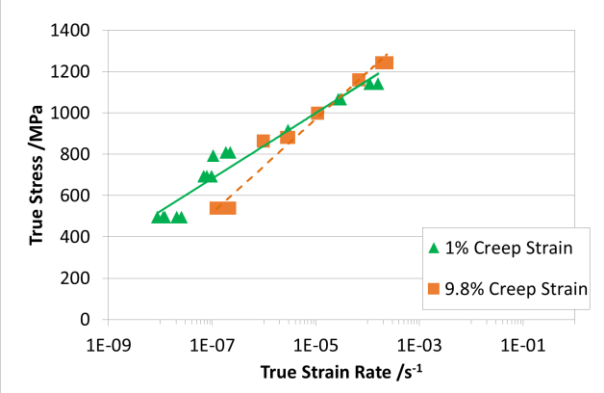

Figure 2 - Typical relationship between instantaneous strain rate and stress for two levels of creep strain at 700°C

The linear relationship demonstrated provides a framework for building a model for the creep rate as a function of stress and strain, see equation (3). The variables *A* and *B* will be defined as functions of creep strain. This relation can be inverted to show that the strain rate ($\dot{\varepsilon}$) increases exponentially with stress.

$$\sigma = A\, ln(\dot{\varepsilon}) + B \tag{3}$$

Although this framework holds for finite stresses, it predicts a non-zero strain rate at zero stress. A correction can be applied by including an offset to the strain rate equal to the rate predicted at zero stress. This correction is small enough that it can be considered negligible in the stress range under study. Equation (4) therefore provides a representation of the creep behaviour shown in Figure 2 whilst providing consistent zero stress behaviour. The trend described by Equation (4) is expected to hold during tertiary creep only, i.e.: after primary creep has completed and before the deformation becomes heterogeneous.

$$\sigma = A\, ln\left(\dot{\varepsilon} + e^{\frac{-B}{A}}\right) + B \tag{4}$$

The parameters *A* and *B* were determined for five levels of strain by fitting to a set of creep tests performed at 700°C. The fitting process was carried out using the Solver function in Microsoft Excel. The resulting values for these parameters are shown in Figure 3. Both parameters appear to indicate a linear relationship with strain, which suggests a simple method for fitting to a larger set of data points is possible.

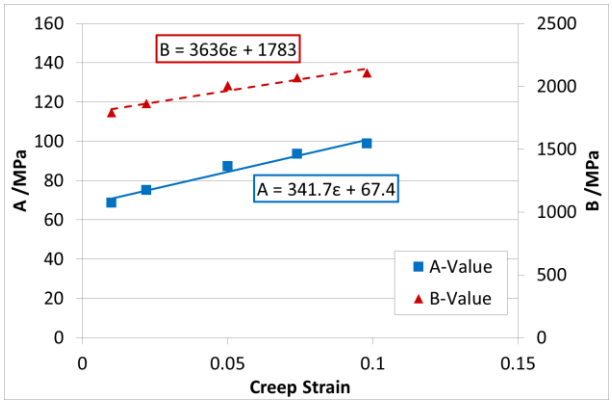

Figure 3 – Relationship between the parameters 'A' and 'B' and creep strain

The parameters *A* and *B* can therefore be described by equations (5) and (6). The linear assumption is a simplification, but it was taken to be suitable for the purposes of this paper.

$$A = A'\varepsilon + A° \tag{5}$$

$$B = B'\varepsilon + B° \tag{6}$$

To confirm whether the linear relationship between the parameters *A* and *B* and the current creep strain allows the model to recreate creep rate evolution accurately, the model has been integrated under conditions of constant load, and the rate as a function of strain plotted in Figure 4. The model is plotted alongside experimental data for a creep test performed at 700°C under an initial applied stress of 500MPa. The resultant curve in Figure 4 demonstrates that the model can recreate the rate evolution reasonably well, if the effects of primary creep are ignored. The predicted curve does not match the strain rate evolution exactly due to the inherent scatter within the original dataset. It does however, confirm that the overall curve shape is replicated reasonably well, as the magnitude is maintained at approximately half that seen experimentally.

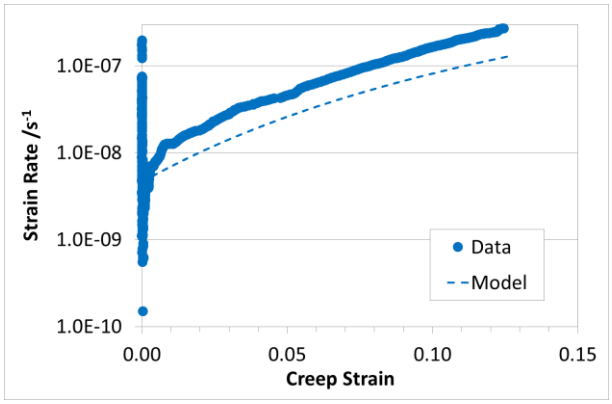

Figure 4 – Typical creep curve for RR1000 at 700°C under an initial applied stress of 500MPa

4.2 Primary Creep

The model described by equation (4) is able to replicate the shape of the creep curve during tertiary creep. The effects of primary creep are to be produced by lowering the stress response, such that the material is softened at low strains. This is achieved by multiplying the stress response by a value smaller than one.

The primary term is based on an exponential decay equation, which reaches a negligibly small value after the effects of primary creep are no longer expected. Modelling primary creep in this way is similar to the primary term in the theta-projection method[2], except that the primary variable here is strain and not time. The form of the primary softening term is shown by equation (7). The basic model, capable of replicating primary and tertiary creep is shown by equation (8). This is produced by multiplying equations (4) and (7).

$$C = 1 - C_0 \, e^{-C_1 \varepsilon^C} \tag{7}$$

$$\sigma = \left[A \, ln\left(\dot{\varepsilon} + e^{\frac{-B}{A}} \right) + B \right] \cdot C \tag{8}$$

The parameter C_0 controls the strength of the softening effect and C_1 controls the rate at which the effect of the term decays. Due to the difficulty of accurately measuring the strain rate at the start of a creep test, C_0 is to be determined by fitting to the creep curves. The parameter C_1 can be estimated by measuring the strain to minimum rate and using this to guide the rate at which the primary term decays.

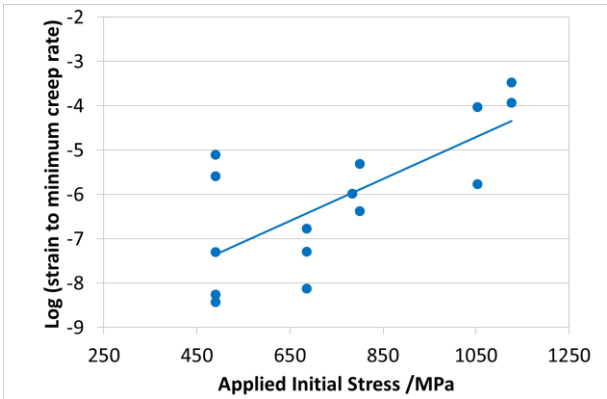

Figure 5 - Strain to minimum rate shown as a function of the initial applied creep stress.

The relationship between strain to minimum rate and the applied initial stress during a creep test is shown by Figure 5. The data contains a significant amount of scatter due to the methods used to the record the original creep data. It is presumed that this scatter is a result of the difficulty in measuring the small strains associated with primary creep. The strain to minimum rate can be seen to increase with applied stress. The y-axis on the chart shows the log of strain to minimum rate and therefore the relationship between the two can be expressed by an exponential function. The resultant equation for the strain to minimum rate is shown by equation (9), where *I* and *J* are taken from Figure 5. *J* is equal to the slope of the straight line and *I* is *e* (the base of the natural log) to the power of the gradient.

$$\varepsilon_{MinRate} = I \cdot e^{JS} \tag{9}$$

By assuming the strain to minimum rate represents a sensible cut-off point for the primary softening term, the value for C_1 can be estimated. If the exponential term in equation (7) reaches a small value at the strain to minimum rate, then the value for C_1 is determinable by rearranging the exponential

term. The value is arbitrarily taken as 0.1 for all further calculations. Equation (11) shows the resultant equation for C_1, where the parameter *I** is introduced to simplify the equation.

$$0.1 = e^{-C_1 \cdot \varepsilon_{MinRate}} = e^{-C_1 \cdot I \cdot e^{JS}} \quad \mathbf{0.1} = e^{-C_1 \varepsilon_{MinRate}} = e^{-C_1 \cdot I \cdot e^{JS}} \tag{10}$$

$$C_1 = \frac{-ln(0.1) \cdot e^{-JS}}{I} = I^* \cdot e^{-JS} \tag{11}$$

The full creep model is constructed by combining equations (7), (8) and (11), to produce equation (12). This equation is therefore capable of recreating the shape of a creep curve from initial loading up until heterogeneous deformation begins. Due to the inclusion of the primary term, the stress parameter is now found on both sides of the equation. This complicates the process of using this model to produce a stress response for a set condition, which is sometimes used to compare the accuracy of a creep model. However, the model is still simple to rearrange, giving the strain rate as a function of loading condition, and this is the required arrangement for adapting the model to a finite element simulation.

$$\sigma = \left[A\, ln\left(\dot{\varepsilon} + e^{\frac{-B}{A}}\right) + B\right] \cdot \left(1 - C_0\, e^{-I^* \times e^{-J\sigma}\varepsilon}\right) \tag{12}$$

The parameter C_1 in equation (7) is derived using the initial applied stress from a range of creep tests. However, the stress parameter in equation (12) is the instantaneous true stress, a value that varies throughout a creep test as a function of accumulated strain. In order to maintain simplicity the initial applied stress in the C-term is replaced with the true stress. Due to the small strains associated with primary creep in RR1000, the difference between the true stress and the engineering stress is negligible during the phase in which the primary term is active.

Equation (12) has been designed such that it can be easily rearranged to produce the instantaneous strain rate, given the current stress-strain condition; see equation (13). This equation can be integrated simply to produce creep curves representing constant load or constant stress tests as required.

$$\dot{\varepsilon} = e^{\frac{1}{A} \times \left(\frac{\sigma}{1 - C_0\, e^{-I^*\, \varepsilon\, e^{-J\sigma}}} - B\right)} - e^{\frac{-B}{A}} \tag{13}$$

5. Results

A comparison has been made between the proposed model and experimentally produced creep curves. Equation (13) was integrated under constant load conditions within a spreadsheet environment. The spreadsheet used included the effects of thermal expansion of the specimen and elastic deformation. The true stress evolution throughout the test was therefore reproduced as faithfully as possible.

The model was compared against a set of three constant load creep tests, all performed at a temperature of 700°C. The three different stresses are chosen to produce significantly different creep curves. The lowest stress used in this comparison is 500MPa. This stress-temperature combination produces a relatively long rupture life, under well understood conditions. The highest stress is

1074MPa, which is set above the material yield stress at this temperature and therefore produces a relatively short rupture life.

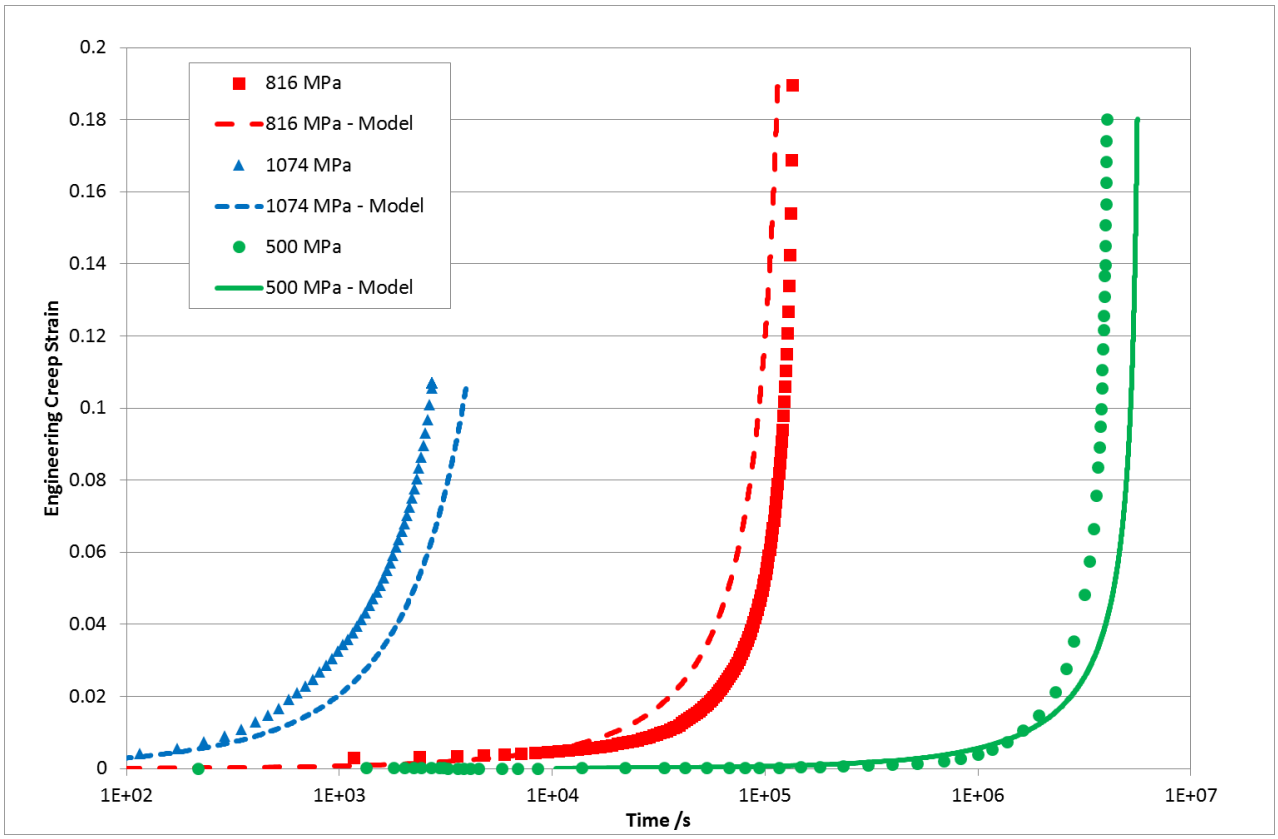

Figure 6 - Comparison between predicted and measured creep behaviours for different stresses at 700°C

The test results are compared with the predictions in Figure 6, with the predictions represented by the lines and the experimental results by the points. The test results demonstrate at least an order of magnitude difference between the rupture times for each stress. The predictions match this behaviour excellently, demonstrating that the model is capable of replicating the creep behaviour over a large range of stresses. The curvature of each prediction matches reasonably with the corresponding test result.

The parameters required to produce the predictions in Figure 6 are shown in Table 1. These were generated utilising the same method as used to produce Figure 3. The numbers produced are different due to the inclusion of primary creep and a greater number of strain points at which values were calculated.

A_1	A_0	B_1	B_0
367.4	69.8	4184	1830
I*	J	C_0	
15143	3.6E-3	0.06	

Table 1 – Model parameters to produce creep curves

To demonstrate the applicability of the model to a range of temperatures, the model has been refitted to experimental data produced at three further temperatures. The extra data was produced at 675, 725 and 750°C. These fits were then used to model the time to 5% creep strain given an initial applied stress. The resulting curves are compared with experimental data in Figure 7, where the lines

represent the predictions and the dots represent test results. It can be seen that the predictions readily align with the measurements suggesting that the model is not restricted to use at a single temperature.

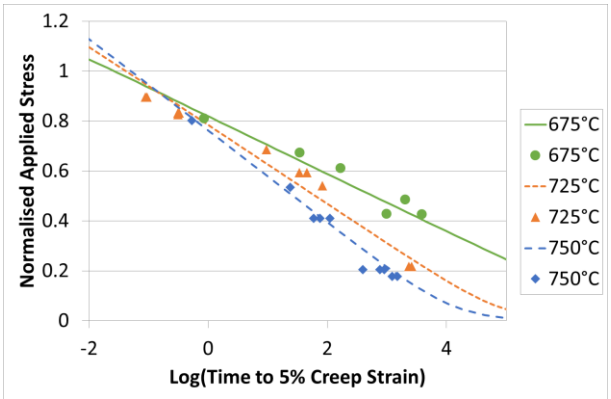

Figure 7 – Normalised stress versus time to 5% creep strain for RR1000 at 675, 725 and 750°C.

6. Discussion and Finite Element Application

The proposed creep model was implemented in a finite element model by adapting it to an Abaqus™ user creep routine. The process of adapting the model was relatively simple because the model was designed for use with finite element simulations. The user subroutine is required to provide Abaqus™ with a uniaxial strain rate given the von Mises stress and equivalent creep strain. This value is produced by equation (13) without modification. The Abaqus™ software is capable of implementing an automatic time-stepping process, allowing the run-times to be optimised whilst maintaining solution accuracy. This process requires the definition of the differentials of the strain rate with respect to stress and strain. The derived differentials are shown by equations (14) and (15).

$$\frac{d\dot{\varepsilon}}{d\sigma} = \frac{e^{\left(\frac{\sigma}{AC}-\frac{B}{A}\right)}}{A}\cdot\left[\frac{1}{C}+\frac{\sigma I^{*} J \varepsilon e^{-J\sigma}(1-C)}{C^{2}}\right] \tag{14}$$

$$\frac{d\dot{\varepsilon}}{d\varepsilon} = e^{\left(\frac{\sigma}{A\cdot C}-\frac{B}{A}\right)}\cdot\left[\left(\frac{-\sigma\left(A_1 C + A I^{*} e^{-J\sigma}(1-C)\right)}{A^{2}C^{2}}\right)-\left(\frac{B_1}{A}-\frac{A_1 B}{A^{2}}\right)\right]+e^{\frac{-B}{A}}\cdot\left(\frac{B_1}{A}-\frac{A_1 B}{A^{2}}\right) \tag{15}$$

Equations (13), (14) and (15) were coded in FORTRAN as a user subroutine and applied to a simulation of a creep test. The model used is shown in Figure 8. The specimen, shown by Figure 1, was recreated by a 2d axisymmetric mesh representing one half of the specimen. The parallel sections of the specimens were meshed using 8-node brick elements, whilst the curved section uses 6-node triangular elements. The model includes a ridge feature, designed to allow the secure attachment of an extensometer cage across the specimen. This feature was included as it affects the global strain measured across the gauge length.

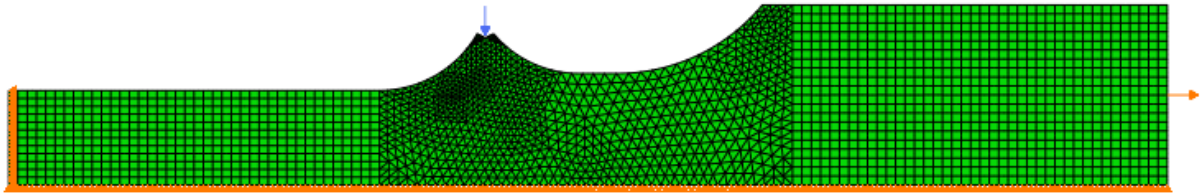

Figure 8 – Finite element model of half specimen showing applied boundaries (orange edges) and gauge measurement location (blue arrow)

The model was set up to use elastic and thermal expansion properties typical for this material. The creep condition was achieved by applying a uniform temperature (of 700°C) and a constant load to the right-hand surface, equal to that applied during the original test (816MPa over a surface area of 19.64mm², or ~16kN). The effects of changing geometry were including by setting the Abaqus™ parameter 'nlgeom' to 'yes'.

The model was run until the engineering strain matched that achieved by the specimen under test. The resultant creep curves are shown by Figure 9. As is common practice for analysing creep tests, the strains were zeroed once the load application was complete to remove any instantaneous strain contributions.

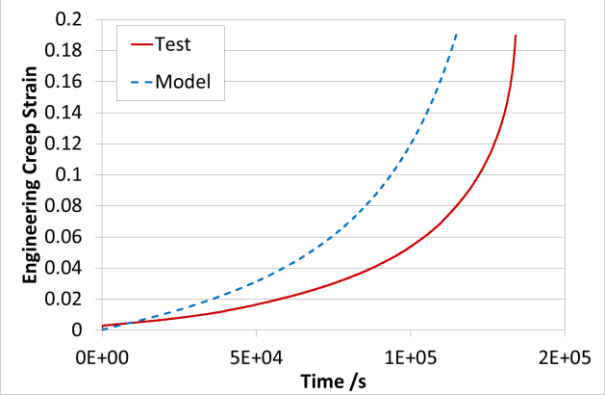

Figure 9 – Comparison of creep curves produced by Abaqus™ model and experiment at 700°C and 816MPa

The creep curves in Figure 9 follow a similar curvature and do not differ significantly in terms of time to the failure strain. The gradients at failure are different, with the test result reaching a slightly higher rate just before reaching the failure strain than seen in the Abaqus™ model. This is attributed to the fact that the Abaqus™ model maintains homogenous deformation up to this point, whilst the test specimen showed signs of necking upon post-test examination.

The creep model recreated the creep behaviour expected and presented no difficulties in terms of model stability. The model was able to maintain a consistent time step for the majority of the simulation. The current implementation of the creep model requires a small time-step to allow successful completion of the model. This resulted in run times of approximately 2 hours. It is expected that this can be decreased by relaxing the time control settings within Abaqus™, although this would require a sensitivity study to ensure no accuracy is lost.

7. Conclusions

- A creep model has been presented, which is based upon the true-stress true-strain interpretation of a set of constant load creep tests.
- The effects of primary creep are included through an assumed relationship between the strain to minimum rate and the applied engineering stress.
- The model is demonstrated to replicate creep curves using reasonably simple, numerical integration techniques over a large stress range.
- It has been demonstrated that the model is easily adaptable as a user defined creep model in the finite element package Abaqus™. This suggests that the model would also apply to other finite element software, as the standard format for user models is often similar.

8. Acknowledgments

The authors would like to thank the EPSRC for funding and also Rolls-Royce Plc. for additional funding and providing experimental test data in support of this work.

9. References

1. Garofalo, F.: '*Fundamentals of creep and creep rupture in metals'; 1965,* New York : MacMillan, Inc.

2. Evans, R. and Wilshire, B.: '*Creep of metals and alloys'; 1985,* London : Institution of Metals

3. Sinha, Nirmal K.: '*Constant-load tertiary creep in nickel-base single crystal superalloys'*, Materials Science and Engineering A, 2006, **432**, 129-141.

4. Ng, L. and Zarrabi, K.: '*On Creep Failure of Notched Bars',* Engineering Failure Analysis, 2008, **15**, 774-786.

5. Norton, F.: *'The creep of steel at high temperatures'; 1929,* London : McGraw-Hill

6. Dyson, B. F. and McLean, M.: *'Particle Coarsening, σ_o and Tertiary Creep',* Acta Metallurgica, 1983, **31**, 17-27.

7. Whittaker, M.T., Evans, M. and Wilshire, B.: '*Long-term creep data prediction for type 316H stainless steel',* Materials Science and Engineering A, 2012, **552**, 145-150.

8. Whittaker, M.T. and Wilshire, B.: '*Advanced Procedures for Long-Term Creep Data Prediction for 2.25 Chromium Steels',* Metallurgical and Materials Transactions A, 2013, **44A**, 136-153

9. Esposito, L. and Bonora, N.: '*Time-independent formulation for creep damage modelling in metals based on void and crack evolution',* Materials Science and Engineering A, June 2009, **510**, 207-213

10. Dyson, B. and McLean, M.: *'Microstructural evolution and its effects on the creep performance of high temperature alloys',* Microstructural stability of creep resistant alloys for high temperature applications, 1998, 371-393.

11. Manonukul, A., Dunne, F.P.E. and Knowles, D.: '*Physically-based model for creep in nickel-base superalloy C263 both above and below the gamma solvus',* Acta Materialia, 2002, **50**, 2971-2931

12. '*Metallic materials - Uniaxial creep testing in tension - Method of test (ISO 204:2009)',* BS EN ISO 204:2009